

Characteristics of strong ferromagnetic Josephson junctions with epitaxial barriers

C. Bell,^{1,*} R. Loloee,² G. Burnell,¹ and M. G. Blamire¹

¹*Materials Science Department, IRC in Superconductivity and IRC in Nanotechnology, University of Cambridge, Cambridge, United Kingdom*

²*Department of Physics and Astronomy, Center for Sensor Materials and Center for Fundamental Material Research, Michigan State University, East Lansing, Michigan 48824, USA*

(Received 22 February 2005; published 4 May 2005)

We present the measurement of superconductor/ferromagnetic Josephson junctions, based on an epitaxial Nb bottom electrode and epitaxial Fe₂₀Ni₈₀ barrier. Uniform junctions have been fabricated with a barrier thicknesses in the range 2–12 nm. The maximum critical current density $\sim 2.4 \pm 0.2 \times 10^9$ Am⁻² was found for a device with a 3-nm-thick barrier at 4.2 K, corresponding to an average characteristic voltage $I_C R_N \sim 16$ μ V. The $I_C R_N$ showed a nonmonotonic behavior with Fe₂₀Ni₈₀ thickness. The variation of the resistance of a unit area AR_N , of the junctions with barrier thickness gave a Nb/Py specific interface resistance of 6.0 ± 0.5 f Ω m² and Fe₂₀Ni₈₀ resistivity of 174 ± 50 n Ω m, consistent with other studies in polycrystalline samples.

DOI: 10.1103/PhysRevB.71.180501

PACS number(s): 74.45.+c, 72.25.Mk, 75.70.Cn

I. INTRODUCTION

The early research into the proximity effect between superconductors (S) and ferromagnets (F) concentrated on measurements of the critical temperature T_C and critical field of S/F heterostructures. A motivating factor for this research was the realization of the π state, in which the ground-state phase difference between S layers changes from 0 to π , due to the oscillation of the superconducting order parameter induced in the F layer.¹ The transition should manifest itself as a nonmonotonic change in the properties of the multilayers, as a function of F layer thickness d_F . Many epitaxial and polycrystalline systems of materials were investigated, using various growth techniques. Although oscillatory $T_C(d_F)$ were observed (see Ref. 2 for a review), these studies were complicated by interface effects and “dead” magnetic layers at the S/F interface, which made the interpretation of the T_C data more difficult.³

It was not until the measurement of current perpendicular to plane (CPP) Josephson junctions with ferromagnetic barriers (S/F/S) that the π shift could be conclusively demonstrated. Such π junctions have been characterized as a function of temperature and d_F (Refs. 4 and 5), using alloys whose composition could be tuned to achieve an appropriately low Curie temperature (T_M), such that the $0-\pi$ crossover could be observed in a suitable window of experimental phase space. These π junctions have since been incorporated into loop geometries to further demonstrate the π shift.^{6,7} S/F/S junctions have also been fabricated with the relatively high T_M ferromagnets Ni (Ref. 8), Co (Ref. 9), and composite Co/Cu/Fe₂₀Ni₈₀ structures.¹⁰ In these cases the junctions are much more sensitive to the barrier properties and d_F , and hence the $0-\pi$ crossover has not been clearly demonstrated.

In all of the above CPP junctions, the S and F layers have been polycrystalline and in the dirty limit. The realization of epitaxial junctions in the clean limit may remove some of the difficulties of measuring low T_M alloy systems (which are sensitive to stoichiometry and harder to characterize magnetically), as well as the sensitivity to d_F of the high T_M

barriers. Clean limit junctions are also expected to show a nonsinusoidal current-phase relationship,¹¹ in contrast to recent measurements of S/F/S junctions with Cu_xNi_{1-x} alloy barriers.¹² S/F/S π junctions have been proposed as potential logic elements in quantum computing circuits;^{13,14} however, the present critical current—resistance product ($I_C R_N$) values are relatively small at present. The clean limit may again provide a route to achieving much higher critical current densities J_C , and hence $I_C R_N$. All of these factors motivates the investigation of epitaxial S/F/S junctions. The epitaxial Fe₂₀Ni₈₀ (Py) system is also of interest in spintronic applications, such as ballistic spin valves and spin torque devices, and also provides an interesting comparison to the studies of polycrystalline Nb/normal-metal (N) and F/N interfaces.¹⁵⁻¹⁷

II. FILM GROWTH AND CHARACTERIZATION

Our (1 $\bar{1}0$) Nb/(111) Fe₂₀Ni₈₀ (Py) films are grown by sputtering on (11 $\bar{2}0$) Al₂O₃ as described in detail elsewhere.¹⁸ To improve the epitaxy and reduce the strain in the films, the heterostructure is Nb/Cu/Py/Cu/Nb with the thicknesses of the two Cu layers ~ 5 nm, [with (111) orientation]. The Cu layers are expected to be strongly proximitized by the Nb electrodes and should not significantly reduce the J_C of the devices. The Py thickness d_{Py} , was in the range 2–12 nm. The samples with $d_{Py}=2, 4,$ and 6 nm were initially grown with a bottom Nb layer of thickness 200 nm, and a top electrode of 20 nm of Nb followed by a 5-nm Au capping layer. This Au was removed *ex situ* by Ar ion milling, and the top Nb electrode deposited by dc sputtering. All of the remaining samples were grown in a second deposition, with the top and bottom Nb thicknesses of ~ 250 nm, deposited *in situ*. To achieve epitaxy, the Py barrier was grown at 423 K, and the Nb at 1023 K. It was not possible therefore to grow the top Nb layer epitaxially at the reduced temperatures required for the Cu and Py layers.

Figure 1 shows the x-ray diffraction peaks of the Nb, Cu, and Py layers in the $d_{Py}=6$ nm sample (taken with CuK α

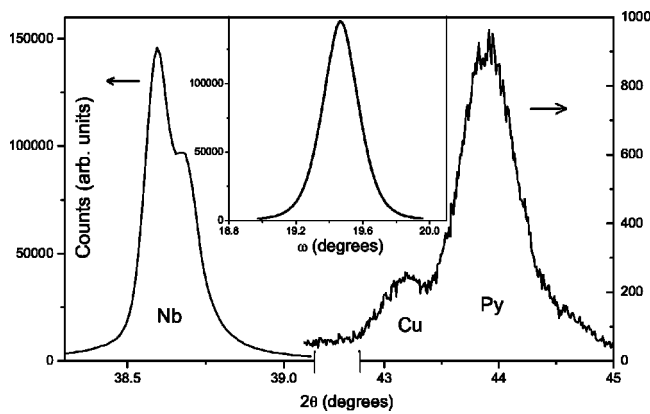


FIG. 1. X-ray diffraction scan of $(1\bar{1}0)$ Nb, (111) Cu, and (111) Py peaks at positions $2\theta=38.6^\circ$, 43.2° , and 43.9° , respectively. The splitting of the Nb peak is caused by the presence of the two $\text{CuK}\alpha$ radiation lines. Inset: An ω scan of the primary Nb peak.

radiation using a Philips X'Pert powder diffractometer). The full width at half maximum values obtained from ω scans were $\sim 0.25^\circ$ for the Nb layer (inset of Fig. 1), and $\sim 0.78^\circ$ for the Py layer (not shown). This confirms the epitaxial nature of the bottom electrode and barrier. A resistance versus temperature, $R(T)$, measurement of the unpatterned $d_{\text{Py}}=2$ nm film (before further Nb was deposited, such that the relatively thick epitaxial Nb layer dominates the conductivity) was also made. The film showed a residual resistance ratio $R(T=10\text{ K})/R(T=300\text{ K})=14.2$. This is of similar order to other epitaxial Nb films, in which the superconducting coherence length $\xi_S=18$ nm (Ref. 19), compared to a dirty limit value of ~ 6 nm in polycrystalline sputtered films.²⁰

The magnetic properties were characterized with a vibrating sample magnetometer at room temperature. Figure 2 shows the saturation moment per unit area of the films in this study (along with a typical hysteresis loop shown in the inset). Extrapolating the least-squares fit gives a nominal magnetically “dead” layer of thickness ~ 7 Å.

The films were patterned using optical lithography, followed by broad beam Ar ion milling (1 mA cm^{-2} , 500 V) to

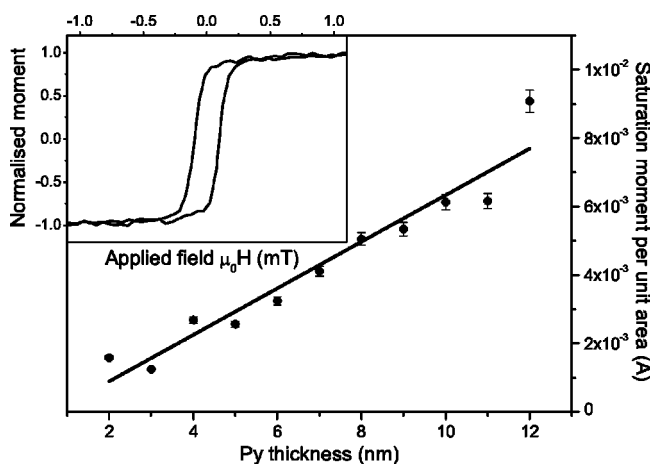


FIG. 2. Scaling of the magnetic moment per unit area vs Py thickness. The line is a least-squares fit to the data. Inset: Hysteresis loop of the 2-nm Py film at 295 K.

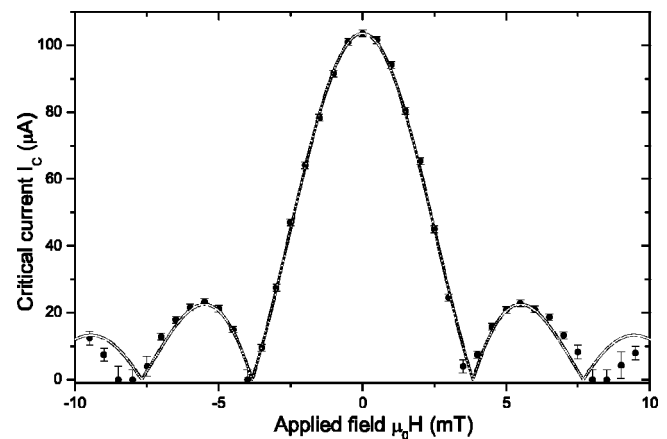


FIG. 3. $I_C(H)$ modulation for a device demagnetized at 4.2 K for a 2-nm-thick Py barrier. The device dimension in the direction perpendicular to the applied field is $\sim 1.06\ \mu\text{m}$. The line is a best fit to a “Fraunhofer” function.

micron scale wires and associated tracks and contact pads, to allow four-point measurements to be performed. These tracks were then processed in a Ga^+ focused ion beam to achieve vertical transport with a device area in the range $0.05\text{--}1.1\ \mu\text{m}^2$. This process is described in detail elsewhere²¹ and has been used previously to fabricate Josephson junctions with ferromagnetic barriers.¹⁰ Transport measurements were made in a liquid He dip probe. The differential resistance as a function of bias current of the junction was made with a lock-in amplifier, and the I_C found using a resistive criterion. The R_N was measured using a quasi-dc bias current of 3–5 mA. This enabled the nonlinear part of the I - V near I_C to be neglected, but was not too large to drive the Nb electrodes normal.

III. RESULTS AND DISCUSSION

An $I_C(H)$ modulation obtained in a junction with lateral area $\sim 1060 \times 250\text{ nm}^2$ is shown in Fig. 3. In this case the field is applied in the direction perpendicular to the larger dimension of the device. It is expected that the coercive field of the Py should increase relative to that taken from the room-temperature hysteresis loop shown in Fig. 2, due to the reduced temperature and the aspect ratio of the submicron device.²² In this case the applied field required to modulate the I_C does not significantly affect the magnetization of the Py, and the $I_C(H)$ is symmetric about zero field. The good fit to the ideal “Fraunhofer” pattern indicates a uniform current flow in the junction. We note, however, that the effective magnetic area of the junction is larger than expected. This effect has been observed in other junctions with this geometry¹⁰ containing Py, and may be due to flux focusing from the nearby electrodes. Relatively smaller junctions, which require larger fields to modulate the I_C , were found to show hysteresis which we associate with changes in the Py magnetization. This results in net induction in the barrier, which shifts the $I_C(H)$ pattern away from $H=0$ and reduces the I_C at zero field from its true maximum value.²³

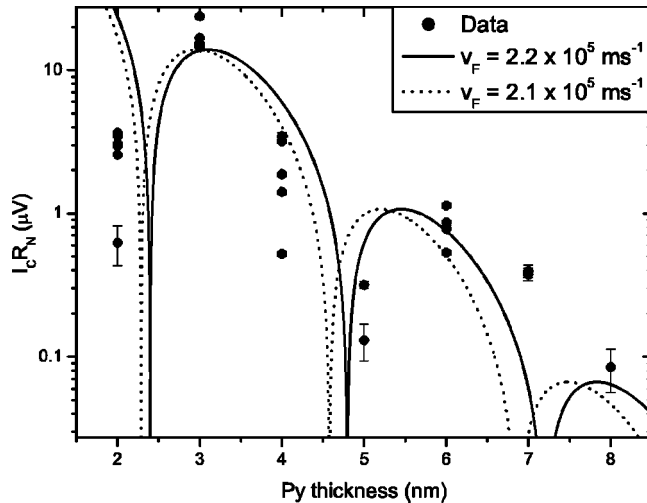


FIG. 4. Characteristic voltage $I_C R_N$ as a function of Py thickness at $T=4.2$ K. The dashed and solid lines are two fits to Eq. (1), as described in the text.

To avoid falsely small values of I_C , the films were demagnetized at 4.2 K, as well as the $I_C(H)$ pattern being directly measured where possible (for devices with $I_C R_N > 2 \mu\text{V}$). In some cases however, the offset of the maximum I_C from $H=0$ could not be removed. The cause of this is ascribed to shape anisotropy in the submicron devices which provides an additional demagnetizing field which may prevent the formation of a flux-closed domain structure in the barrier.

The variation of $I_C R_N(d_{\text{Py}})$ is shown in Fig. 4. Other devices showed much larger J_C values, but showed strongly distorted or no $I_C(H)$ modulation, implying shorting at the edges of the junctions due to redeposition during device fabrication. For $d_{\text{Py}} > 8$ nm the devices showed some reduction of the differential resistance around $I=0$, but did not show a measurable supercurrent at $T=4.2$ K (this was also the case in several devices with $d_{\text{Py}}=7$ and 8 nm). No reentrant $I_C R_N$ was observed up to $d_{\text{Py}}=12$ nm. It is clear that there is a strong suppression of $I_C R_N$ for increasing d_{Py} , but despite some scatter in the data of Fig. 4 for each set of devices with constant d_{Py} , the decay is clearly not purely exponential. A component of this nonmonotonic change may be associated with the slightly different preparation methods of the 2-, 4-, and 6-nm-thick barriers, or run-to-run variation in the system. For example for $d_{\text{Py}}=3$ nm, the fully *in situ* deposition may imply a higher quality and larger $I_C R_N$, however this is inconsistent with the same comparison between the samples with $d_{\text{Py}}=4, 5$, and 6 nm. Therefore the variation in $I_C R_N$ would seem to be a true effect associated with the oscillatory induced superconducting order parameter in the Py layer.

We can compare this behavior to the nonepitaxial evaporated junctions of Blum *et al.*,⁸ with the structure Nb/Cu/Ni/Cu/Nb. In that case a measurable critical current at $T=4.2$ K was observed up to a Ni thickness of 9 nm—similar to the present data. Due to the relatively small number of data points and the scatter, it is difficult to accurately fit this nonmonotonic decay. We model the data using

$$I_C R_N \propto |\sin(2E_{\text{ex}} d_F / \hbar v_F)| / (2E_{\text{ex}} d_F / \hbar v_F), \quad (1)$$

where v_F is the Fermi velocity of Py, and E_{ex} the exchange energy.^{1,8} These two parameters have recently

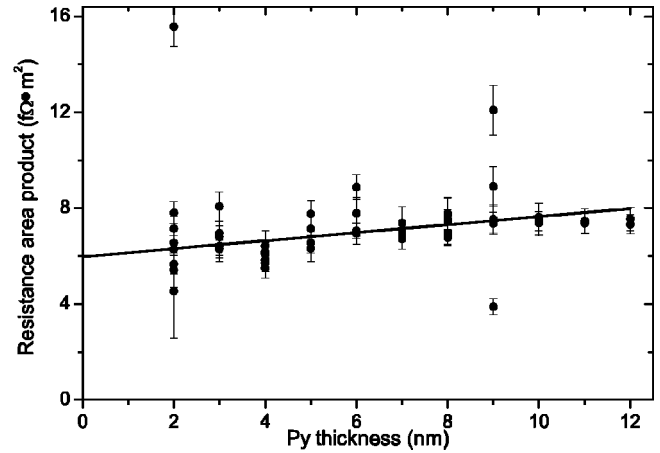


FIG. 5. Resistance area product (AR_N) at $T=4.2$ K as a function of Py thickness. The line is a best fit excluding the point with the largest AR_N for $d_{\text{Py}}=2$ nm.

been measured²⁴ in Py as $E_{\text{ex}}=135$ meV and $v_F=2.2 \pm 0.2 \times 10^5$ ms⁻¹ (for the majority spin). The lines in Fig. 4 correspond to $E_{\text{ex}}=95$ meV, with both $v_F=2.2$ and 2.1×10^5 ms⁻¹, to indicate the degree of variation the error in v_F causes. The agreement between the data and the model is not ideal, however for an order of magnitude estimate it is clear that the fit is acceptable. The period of oscillation of $I_C R_N(d_F)$ is given by $\pi \hbar v_F / E_{\text{ex}}$, and can therefore be estimated to be of the order of 5 nm, again similar in magnitude to the 5.4-nm value obtained by Blum *et al.*⁸ We note that these junctions fall in a regime for which Eq. (1) will not be valid for large d_{Py} , however the uncertainty in parameters such as v_F do not allow accurate modeling without a fuller characterization of the Py films, and a complete theoretical model. For the previously mentioned Ni junctions,⁸ a maximum $I_C \sim 20$ mA was observed at $T=4.2$ K in $10 \times 10 \mu\text{m}^2$ devices for a 1-nm-thick Ni barrier, giving $J_C=2 \times 10^8$ Am⁻². In our samples, one device with $d_{\text{Py}}=3$ nm had $I_C=1.03$ mA with a lateral area of $0.35 \pm 0.02 \mu\text{m}^2$, giving the highest $J_C \sim 2.9 \pm 0.2 \times 10^9$ Am⁻² at the same temperature, the average for $d_{\text{Py}}=3$ nm was $J_C=2.4 \pm 0.2 \times 10^9$ Am⁻². The larger J_C for the epitaxial films can be attributed to the increased ξ_S of the Nb bottom electrode.

Finally, we have measured the total resistance (R_N) of a unit area AR_N , of all junctions. The variation of AR_N versus d_{Py} over the range of $2 \text{ nm} < d_{\text{Py}} < 12$ nm are shown in Fig. 5. Here AR_N is the total specific resistances; consisting of the specific resistance of the S/F interfaces ($AR_{\text{Nb/Py}}$) in the S/F/S sandwich and the ferromagnetic layer,¹⁵ such that

$$AR_N = 2AR_{\text{Nb/Py}} + \rho_{\text{Py}} d_{\text{Py}}. \quad (2)$$

If we exclude one of the data points (with the highest AR_N for $d_{\text{Py}}=2$ nm), the best fit straight line to our data gives an ordinate intercept of $2AR_{\text{Nb/Py}}=6.0 \pm 0.5$ f Ω m² and the resistivity $\rho_{\text{Py}}=174 \pm 50$ n Ω m (from the slope). The values fall within the range of $2AR_{\text{Nb/Py}}=6-7.5$ f Ω m² and $\rho_{\text{Py}}=110-140$ n Ω m reported for polycrystalline samples.^{15,17}

IV. SUMMARY

We have measured the Josephson current through an epitaxial Py barrier and observed high quality junction characteristics. The $I_C R_N(d_{\text{Py}})$ showed a nonmonotonic behavior, which could be approximately modeled with a simple model. We observed no sign of a reentrant I_C above $d_{\text{Py}}=8$ nm. While suggestive of $0-\pi$ crossovers, we emphasize that without phase-sensitive tests, these oscillations of $I_C R_N$ cannot be shown directly to correspond to such crossovers. The data extracted from the $AR_N(d_{\text{Py}})$ product was consistent with polycrystalline samples.

Although interesting for spin-valve junctions, Py is not an ideal material in which to examine ferromagnetic Josephson junctions in the clean limit, since the spin-diffusion length is relatively short.^{16,24} A reduced spin-diffusion length can have a strong influence on the possible realization of π junctions formed by the interference of multiple Andreev reflection processes at the S/F interfaces. The role of different reflection amplitudes for the minority and majority spins, and the

spin polarization, have been considered elsewhere.^{25,26} Other effects on the Josephson current due to the shape of the Fermi surface in the epitaxial barrier also must be considered, in an analogous fashion to tunnel junctions,²⁷ as well as the effect of spin memory loss due to spin-orbit scattering or spin flipping. The use of elemental, or other epitaxial F layers—with longer spin-diffusion lengths—may allow further increases of the J_C to be achieved, and rule out problems associated with loss of spin memory. With suitable materials and growth technique, the fully epitaxial S/F/S would also be an important system to study.

ACKNOWLEDGMENTS

We thank J. Aarts, E. J. Tarte, C. W. Leung, W. P. Pratt, and J. Bass for useful discussions and assistance. We acknowledge the support of the Engineering and Physical Sciences Research Council UK, the U.S. NSF Grant No. 98-09688, and the European Science Foundation π -shift network.

*Present address: Kamerlingh Onnes Laboratory, Universiteit Leiden, Leiden, The Netherlands. Email address: bell@physics.leidenuniv.nl

- ¹A. I. Buzdin, L. N. Bulaevskiĭ, and S. V. Panyukov, *Pis'ma Zh. Eksp. Teor. Fiz.* **35**, 147 (1982) [*JETP Lett.* **35**, 178 (1982)].
- ²Y. A. Izyumov, Y. N. Proshin, and M. G. Khusainov, *Usp. Fiz. Nauk* **172**, 113 (2002) [*Phys. Usp.* **45**, 109 (2002)].
- ³J. Aarts, J. M. E. Geers, E. Brück, A. A. Golubov, and R. Coehoorn, *Phys. Rev. B* **56**, 2779 (1997).
- ⁴V. V. Ryazanov, V. A. Oboznov, A. Y. Rusanov, A. V. Veretennikov, A. A. Golubov, and J. Aarts, *Phys. Rev. Lett.* **86**, 2427 (2001).
- ⁵T. Kontos, M. Aprili, J. Lesueur, and X. Grison, *Phys. Rev. Lett.* **86**, 304 (2001).
- ⁶V. V. Ryazanov, V. A. Oboznov, A. V. Veretennikov, and A. Y. Rusanov, *Phys. Rev. B* **65**, 020501(R) (2001).
- ⁷A. Bauer, J. Bentner, M. Aprili, M. L. Della-Rocca, M. Reinwald, W. Wegscheider, and C. Strunk, *Phys. Rev. Lett.* **92**, 217001 (2004).
- ⁸Y. Blum, A. Tsukernik, M. Karpovski, and A. Palevski, *Phys. Rev. Lett.* **89**, 187004 (2002).
- ⁹C. Sürgers, T. Hoss, C. Schönenburger, and C. Strunk, *J. Magn. Magn. Mater.* **240**, 598 (2002).
- ¹⁰C. Bell, G. Burnell, C. W. Leung, E. J. Tarte, D.-J. Kang, and M. G. Blamire, *Appl. Phys. Lett.* **84**, 1153 (2004).
- ¹¹A. A. Golubov, M. Y. Kupriyanov, and E. Il'ichev, *Rev. Mod. Phys.* **76**, 411 (2004).
- ¹²S. M. Frolov, D. J. Van Harlingen, V. A. Oboznov, V. V. Bolginov, and V. V. Ryazanov, *Phys. Rev. B* **70**, 144505 (2004).
- ¹³L. B. Ioffe, V. B. Geshkenbein, M. V. Feigel'man, A. L. Fauchère,

and G. Blatter, *Nature (London)* **398**, 679 (1999).

- ¹⁴J. E. Mooij, T. P. Orlando, L. Levitov, L. Tain, C. H. van der Wal, and S. Lloyd, *Science* **285**, 1036 (1999).
- ¹⁵Q. Yang, P. Holody, R. Loloee, L. L. Henry, W. P. Pratt Jr., P. A. Schroeder, and J. Bass, *Phys. Rev. B* **51**, 3226 (1995).
- ¹⁶W. Park, D. V. Baxter, S. Steenwyk, I. Moraru, W. P. Pratt Jr., and J. Bass, *Phys. Rev. B* **62**, 1178 (2000).
- ¹⁷P. Holody, W. C. Chiang, R. Loloee, J. Bass, W. P. Pratt Jr., and P. A. Schroeder, *Phys. Rev. B* **58**, 12 230 (1998).
- ¹⁸R. Loloee, S. Urazhdin, W. P. Pratt Jr., H. Geng, and M. A. Crimp, *Appl. Phys. Lett.* **84**, 2364 (2004).
- ¹⁹T. Mühge, K. Theis-Bröhl, K. Westerholt, H. Zabel, N. N. Garif'yanov, Y. V. Goryunov, I. A. Garifullin, and G. G. Khaliullin, *Phys. Rev. B* **57**, 5071 (1998).
- ²⁰T. Mühge, K. Westerholt, H. Zabel, N. N. Garif'yanov, Y. V. Goryunov, I. A. Garifullin, and G. G. Khaliullin, *Phys. Rev. B* **55**, 8945 (1997).
- ²¹C. Bell, R. H. Hadfield, G. Burnell, D.-J. Kang, M. J. Kappers, and M. G. Blamire, *Nanotechnology* **14**, 630 (2003).
- ²²A. O. Adeyeye, J. A. C. Bland, C. Daboo, J. Lee, U. Ebels, and H. Ahmed, *J. Appl. Phys.* **79**, 6120 (1996).
- ²³V. V. Ryazanov, *Usp. Fiz. Nauk* **169**, 920 (1999) [*Phys. Usp.* **42**, 825 (1999)].
- ²⁴D. Y. Petrovykh, K. N. Altmann, H. Höchst, M. Laubscher, S. Maat, G. J. Mankey, and F. J. Himpsel, *Appl. Phys. Lett.* **73**, 3459 (1998).
- ²⁵Y. S. Barash and I. V. Bobkova, *Phys. Rev. B* **65**, 144502 (2002).
- ²⁶J. Cayssol and G. Montambaux, *Phys. Rev. B* **71**, 012507 (2005).
- ²⁷J. E. Dowman, M. L. A. MacVicar, and J. R. Waldram, *Phys. Rev.* **186**, 452 (1969).